Clinical and Experimental Obstetrics & Gynecology

Clin. Exp. Obstet. Gynecol. **2025**; 52(12): 44373
https://doi.org/10.31083/CEOG44373

Original Research

Ultrasound-Based Intratumoral and Peritumoral Radiomics to Differentiate Between HER2-Low and HER2-Zero Breast Cancers: Model Construction and Performance Evaluation

Mengna Shao[1], Sijie Mo[2], Zhibin Huang[2], Xiaohan Zou[2], Hongtian Tian[2], Huaiyu Wu[2], Shuzhen Tang[2], Mengyun Wang[2], Jinfeng Xu[1,2], Chenyao Xu[3], Fajin Dong[1,2,*], Liping Mao[3,*]

[1]Department of Ultrasound, The First Affiliated Hospital, Southern University of Science and Technology, Shenzhen People's Hospital, 518020 Shenzhen, Guangdong, China
[2]Department of Ultrasound, Shenzhen People's Hospital, The Second Clinical Medical College, Jinan University, 518020 Shenzhen, Guangdong, China
[3]Department of Ultrasonography, Luoyang Maternal and Child Health Hospital, 471000 Luoyang, Henan, China
*Correspondence: dongfajin@szhospital.com (Fajin Dong); lymlp7002@163.com (Liping Mao)
Academic Editors: Paul J.L. Zhang and Michael H. Dahan
Submitted: 29 June 2025 Revised: 19 September 2025 Accepted: 17 October 2025 Published: 17 December 2025

Abstract

Background: Breast cancer (BC) is a major global malignancy with rising incidence. The lack of effective traditional anti-human epidermal growth factor receptor 2 (HER2) therapies for HER2-low BC underscores the critical need to identify this subtype early. Dynamic contrast-enhanced magnetic resonance imaging (DCE-MRI) radiomics can help to differentiate between HER2-low and HER2-zero BC, although this method has limited contrast and access. Ultrasound (US) is a cost-effective technique, although radiomics research remains limited, and traditional radiomics largely ignores peritumoral value. This study aimed to determine whether intra- and peritumoral radiomic features observed by grayscale US can differentiate between HER2-low and HER2-zero BC. **Methods**: This retrospective diagnostic study enrolled 209 consecutive BC cases from May 2022 to January 2024. These cases were categorized as HER2-low (immunohistochemistry (IHC) 1+/2+, no erythroblastic leukemia viral oncogene homolog 2 (*ERBB2*) fluorescence *in situ* hybridization (FISH) amplification, n = 129) or HER2-zero (IHC 0, n = 80). Patients were age-matched and randomly assigned (block size = 10) to the training (n = 155) and validation (n = 54) cohorts, with predefined exclusion criteria applied (e.g., missing pathological data, poor US quality). After calibration, two experienced radiologists performed blinded manual intratumoral region-of-interest (ROI) segmentation (ITK-SNAP v3.8.0), with interoperator consistency confirmed by immunocytochemistry (ICC) >0.75. Pyradiomics was used to automate the expansion of the 1 mm and 2 mm peritumoral regions, feature extraction, and z-score normalization. Features were filtered via Spearman's correlation, Mann-Whitney U test, and least absolute shrinkage and selection operator (LASSO) regression (10-fold cross-validation for optimal λ). A predictive model for HER2 status was built using LASSO regression (variance inflation factor (VIF) <1.2 to avoid multicollinearity), and the performance of this model was evaluated for accuracy, sensitivity, specificity, receiver operating characteristic (ROC) curves (area under the curve, AUC), calibration curves (Hosmer-Lemeshow test), and decision curve analysis (DCA). A radiomic nomogram integrating radiomic and clinical signatures was evaluated in the validation cohort. Statistical analyses were performed using R v4.2.2 (two-sided $p < 0.05$ for significance). **Results**: The clinical model showed limited discrimination in the test set (AUC = 0.594). A total of 3320 radiomic features were extracted from intratumoral, as well as 1 mm and 2 mm peritumoral regions, with the selection of 30, 19, and 24 features, respectively, via LASSO regression. The intratumoral-only model had AUCs of 0.730 (training) and 0.649 (test), while the intratumoral + 1 mm peritumoral model exhibited enhanced performance (training AUC = 0.852; test AUC = 0.868). The 2 mm peritumoral-integrated model demonstrated a high AUC in the training set (0.918), but poor performance in the test set (AUC = 0.509). A combined model (intratumoral + 1 mm peritumoral features + clinical factors) was used to generate a nomogram (no multicollinearity, VIF: 1.039–1.179) with AUCs of 0.882 (training) and 0.835 (test). The DCA confirmed the clinical utility of the combined model, although the diagnostic performance of the model was slightly lower than that of the intratumoral + 1 mm peritumoral model. **Conclusions**: Combining 1 mm peritumoral radiomics with intratumoral and clinical data improves the discrimination of HER2-low from HER2-zero BC (AUC = 0.882), thus reducing the need for biopsy and assisting with therapy planning. Optimizing peritumoral margins enhances diagnostic accuracy, thereby validating radiomics for BC subtyping.

Keywords: breast cancer; HER2; radiomics; ultrasound

1. Introduction

Breast cancer (BC) is the predominant malignancy in the female population globally, and remains the most frequent cause of cancer-related death among women [1]. BC has considerable negative effects on quality of life and survival, accounting globally for approximately 43.8 million cases within a 5-year prevalence period [2]. Epidemiologic data from 2024 show sustained increases in BC incidence rates across demographic strata [3]. Human epidermal growth factor receptor 2 (HER2)-overexpression is observed in 15% of invasive BCs and correlates with increased metastatic propensity and adverse prognostic trajectories [4]. Current translational research in precision oncology has redefined therapeutic paradigms for HER2-driven malignancies, resulting in significant survival benefits from targeted treatment [5]. HER2 signaling not only drives BC progression, but also crosstalks with estrogen receptor pathways, thereby influencing treatment resistance and metastatic potential [6].

Recent oncopathologic consensus defines the HER2-low phenotypic subset as tumors which demonstrate an immunohistochemical (IHC) staining intensity for HER2 of 1+ or 2+, with concomitant absence of erythroblastic leukemia viral oncogene homolog 2 (*ERBB2*) gene amplification as detected by fluorescent *in situ* hybridization (FISH) [7,8]. The physiological interplay between the mammary gland and the female reproductive system underscores the shared risk factors and pathogenic mechanisms between BC (including HER2-low subtypes) and gynecologic cancers. Recent studies have demonstrated that genetic susceptibility (e.g., breast cancer antigen (*BRCA*) mutations), hormonal dysregulation, and lifestyle factors (e.g., obesity, smoking) contribute to BC pathogenesis and even to secondary primary malignancies [9]. Studies have also shown that traditional anti-HER2 treatment modalities are not effective in the treatment of HER2-low BC [2]. However, clinical data indicate that antibody-drug conjugates such as trastuzumab deruxtecan and trastuzumab duocarmazine might confer benefits to patients with low HER2 expression. Indeed, trastuzumab deruxtecan has demonstrated efficacy in HER2-low BC [10], thus expanding the scope of treatment beyond traditional HER2-positive tumors [10–12]. Therefore, identifying HER2-low status at an early stage during BC disease progression is of paramount importance for customizing treatment strategies, particularly in the case of therapy-resistant, hormone receptor-negative tumors [13,14].

Although ultrasound (US) is sensitive for the detection of BC [15], the ability to differentiate between HER2-low and HER2-zero expression continues to pose a significant challenge. Dynamic contrast-enhanced magnetic resonance imaging (DCE-MRI) radiomics has been used to help distinguish between these two BC subtypes [16]. Although Bian *et al*. [17] reported an MRI-based radiomics framework for this differentiation, their methodology is constrained by the need for contrast-enhanced protocols and specialized imaging facilities. Moreover, reliance on core needle biopsies as the principal means for ascertaining HER2 status has proven inadequate, with an approximately 20% rate of misdiagnosis in cases of HER2-low BC [18]. As a primary modality for BC screening, US offers distinct advantages of widespread accessibility and cost-effectiveness compared to MRI. However, despite its clinical significance, there is only limited research on the correlation between US radiomics features and HER2 expression status (HER2-zero vs. HER2-low), with few studies having systematically explored this potential association.

Traditional radiomics analysis has predominantly focused on intratumoral characteristics, largely neglecting the diagnostic potential of peritumoral regions. However, given the heterogeneous invasion patterns observed across different tumor types, where peritumoral areas serve as the primary pathway for tumor infiltration, these regions may provide critical complementary information for tumor diagnosis and characterization [19]. Furthermore, the use of US intratumoral and peritumoral radiomics to differentiate between HER2-low and HER2-zero BC has yet to be reported. The aim of this study was therefore to evaluate the utility of intratumoral and peritumoral radiomic signatures generated by grayscale US in differentiating HER2-low BC from HER2-zero BC.

2. Materials and Methods

The study protocol was approved by the Institutional Review Board of Shenzhen People's Hospital (ethical clearance number: LL-KY-2022479-02) and was conducted in accordance with the principles of the Declaration of Helsinki. All participants provided written informed consent for the use of their clinical and imaging data prior to inclusion in this retrospective study. The study design, execution, and reporting adhered to the rigorous standards of the standards for reporting diagnostic accuracy studies (STARD) guidelines [20] for research into diagnostic accuracy, thereby ensuring transparency, reproducibility, and ethical integrity throughout the investigation.

2.1 Study Population

This retrospective diagnostic study was conducted from May 2022 to January 2024 and enrolled consecutive BC patients (n = 209) who met pre-defined HER2 status criteria. HER2-low (n = 129) was defined as IHC 1+/2+ with no FISH amplification of *ERBB2*, while HER2-zero (n = 80) was defined as IHC 0, as per the 2018 ASCO/CAP guidelines [21]. The cohort was stratified into training (n = 155) and validation (n = 54) subsets through computer-generated block randomization (block size = 10), with mean ages of 52.97 $\pm$ 11.76 and 52.20 $\pm$ 12.46 years, respectively. Covariate balance was maintained through age-matching algorithms. All participants met standardized inclusion criteria through centralized pathology verification.

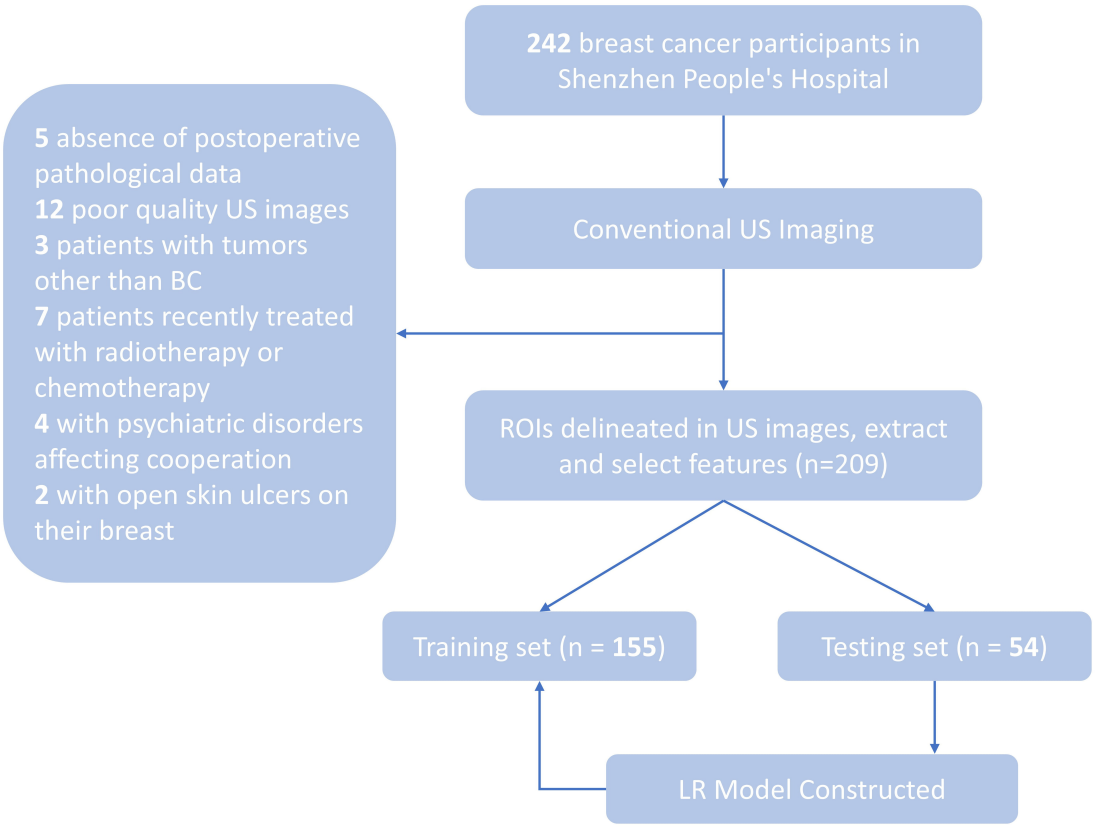

Fig. 1. Flowchart showing inclusion and exclusion criteria. US, Ultrasound; BC, Breast cancer; ROI, region of interest; LR, logistic regression.

Continuous variables were assessed for normal distribution using the Shapiro-Wilk test ($\alpha = 0.05$) and visual inspection of quantile-quantile (Q-Q) plots. Variables with a skewed distribution ($p < 0.05$ on Shapiro-Wilk test) were reported as the median with interquartile range (IQR), while normally distributed variables were reported as the mean $\pm$ standard deviation (SD).

The exclusion criteria were: (1) lack of postoperative pathological data; (2) poor-quality US images; (3) presence of tumor other than BC; (4) BC patients who had received radiotherapy or neoadjuvant chemotherapy within the previous three months; (5) patients with psychiatric disorders that hindered cooperation during clinical examinations; and (6) BC patients with open skin ulcers on the breasts. A flowchart depicting the patient inclusion process is shown in Fig. 1, while Fig. 2 presents a workflow diagram outlining the steps involved in constructing the radiomics model.

2.2 Region-of-Interest (ROI) Segmentation and Feature Extraction

Manual segmentation of tumor regions was conducted with rigorous quality control measures in order to minimize operator-dependent variability. Prior to formal segmentation, each participating radiologist (n = 3) underwent a standardized training program on 15 calibration cases that were excluded from the main study cohort. This training established consensus on critical segmentation parameters, including boundary definition criteria for irregular margins, protocols for handling heterogeneous echo patterns, and standardized ITK-SNAP software settings (version 3.8.0; http://www.itksnap.org/; developed by Paul A. Yushkevich, University of Pennsylvania, Philadelphia, PA, USA). The segmentation process itself involved a dual-observer design with two independent radiologists. Each had more than a decade of specialized experience in breast US, and performed blinded annotations without access to pathological results. To assess interoperator consistency, the immunocytochemistry (ICC) was calculated from 30 randomly selected US images, with ICC values >0.75 indicating satisfactory agreement in ROI delineation. Automated expansion of peritumoral regions (1 mm and 2 mm) was implemented using algorithms from the Pyradiomics package. Radiomic feature extraction and selection were subsequently performed through the Pyradiomics platform (https://pyradiomics.readthedocs.io/en/latest/index.html) to quantify image characteristics.

The radiomic features underwent standardized preprocessing through z-score normalization to eliminate dimensional disparities. Feature correlation analysis was conducted using Spearman's rank correlation coefficient, with highly correlated features (Spearman's $\rho > 0.9$) retained to mitigate multicollinearity. Subsequently, the Mann-

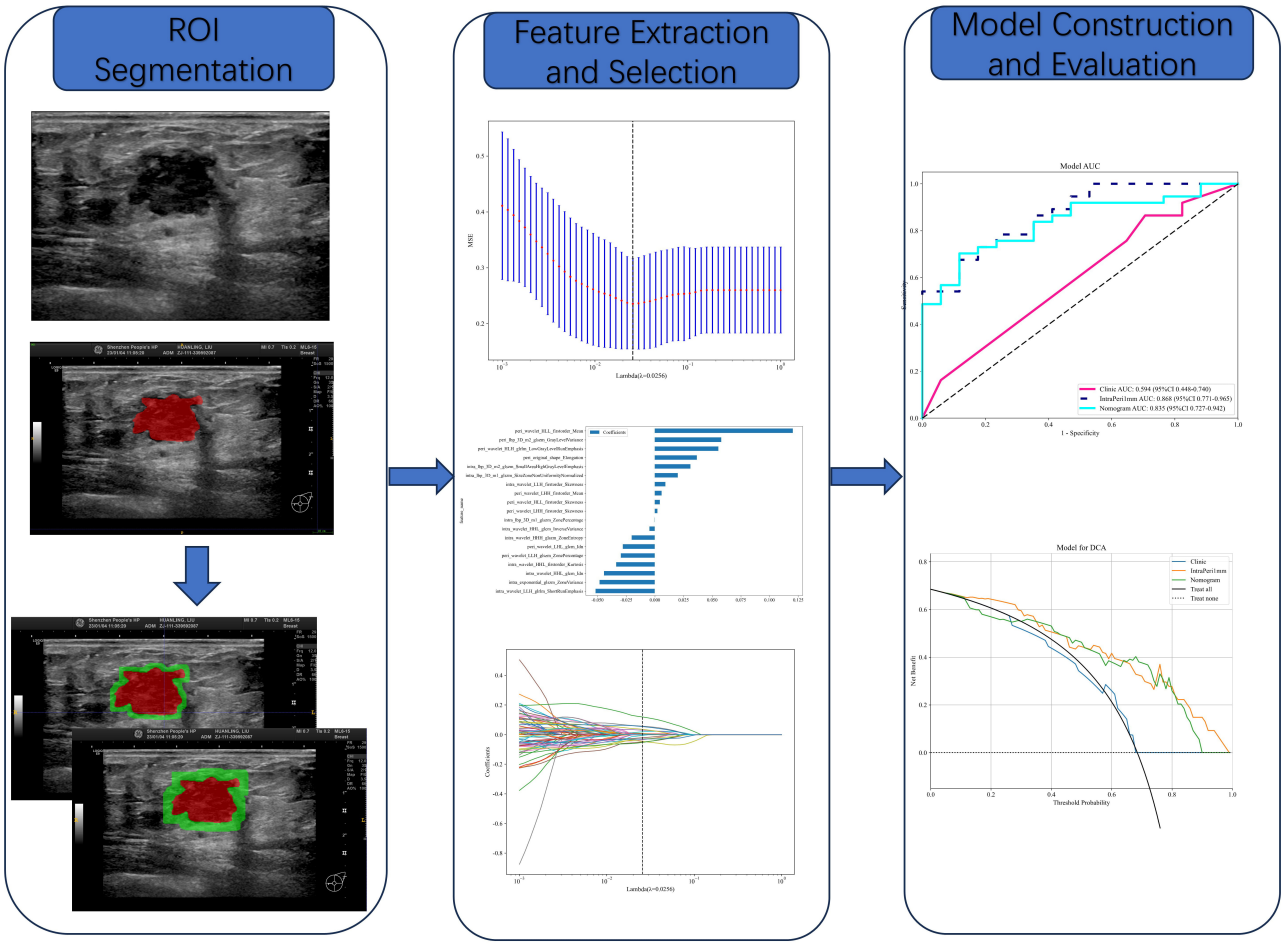

Fig. 2. ROI Segmentation. Note: To define the ROI, manual segmentation was conducted on the intratumoral area in US images, with subsequent AI-assisted automatic segmentation of the peritumoral region at 1 mm and 2 mm intervals. Feature Selection: Features were derived from the delineated US images around the tumor. LASSO regression models were employed to select features, with the aim of enhancing the quality of analysis. Model Construction & Evaluation: Omics models were built based on the selected feature variables, and their diagnostic performance was assessed through analysis by AUC and DCA. AUC, area under the curve; DCA, decision curve analysis; LASSO, least absolute shrinkage and selection operator.

Whitney U test was applied to assess feature discriminative capacity, excluding non-significant features ($p > 0.05$). Final feature selection was carried out via LASSO (least absolute shrinkage and selection operator) regression on the training cohort, where the L1 penalty term automatically nullified non-informative features by driving their coefficients to zero. The optimal regularization parameter λ was determined through 10-fold cross-validation based on minimum criteria, ensuring model generalizability. Features with non-zero coefficients were subsequently incorporated into the logistic regression framework.

2.3 Model Construction and Performance Evaluation

LASSO regression was employed to select variables for the development of a predictive model of HER2 status. Prior to building the predictive model, multicollinearity among variables was assessed by calculating the variance inflation factor (VIF). A VIF value <1.2 indicated that no multicollinearity existed among the final predictors [22]. The diagnostic performance of the model was assessed through metrics including accuracy, sensitivity, and specificity, all of which were obtained from the confusion matrix. A radiomic nomogram was developed by integrating the radiomic signature with the clinical signature. Its diagnostic performance in the test cohort was assessed by plotting receiver operating characteristic (ROC) curves, and the calibration efficiency through calibration curves. The Hosmer-Lemeshow test was applied to gauge the calibration capability of the nomogram, and decision curve analysis (DCA) was performed to determine the clinical utility of the predictive model.

2.4 Statistical Analysis

Statistical analyses were conducted using R software (version 4.2.2; The R Foundation for Statistical Computing, Vienna, Austria). A two-sided p-value of <0.05 was

Table 1. Baseline characteristics of the study cohort.

Variables	Total (n = 209)	HER2-zero (n = 80)	HER2-low (n = 129)	*p*-value
Age (years)	50 (44, 62)	52 (45, 62)	50 (43, 60)	0.414
Height (cm)	158 (155, 161)	158 (154, 161)	158 (155, 161)	0.788
Weight (kg)	57 (55, 60)	58 (54, 60)	57 (55, 60)	0.860
Menopausal status				0.844
Premenopausal	105 (50%)	39 (49%)	66 (51%)	
Postmenopausal	104 (50%)	41 (51%)	63 (49%)	
History of breast cancer				0.745
Absent	199 (95%)	77 (96%)	122 (95%)	
Present	10 (5%)	3 (4%)	7 (5%)	
Location				0.484
Right	102 (49%)	42 (52%)	60 (47%)	
Left	107 (51%)	38 (48%)	69 (53%)	
Clinical tumor stage				0.303
T1	131 (62%)	46 (57%)	85 (66%)	
T2 or above	78 (38%)	34 (42%)	44 (34%)	
Clinical nodal stage				0.439
N0	152 (73%)	61 (76%)	91 (70%)	
N+	57 (27%)	19 (24%)	38 (30%)	
L (mm)	18 (13, 25)	19 (14, 25)	18 (13, 26)	0.944
S (mm)	14 (10, 20)	15 (12, 20)	14 (10, 18)	0.192
Middle (mm)	11 (8, 14)	12 (8, 15)	11 (8, 13)	0.080
Shape				0.383
Oval or Round	1 (0%)	1 (1%)	0 (0%)	
Irregular	208 (100%)	79 (99%)	129 (100%)	
Orientation				0.190
Parallel	48 (23%)	14 (18%)	34 (26%)	
Not parallel	161 (77%)	66 (82%)	95 (74%)	
Margin				<0.001
Not circumscribed	188 (90%)	63 (79%)	125 (97%)	
Circumscribed	21 (10%)	17 (21%)	4 (3%)	
Echo patten				0.222
Hypoechoic	33 (16%)	9 (11%)	24 (19%)	
Others	176 (84%)	71 (89%)	105 (81%)	
Posterior echo				0.600
Shadowing	108 (52%)	39 (49%)	69 (53%)	
No posterior features	101 (48%)	41 (51%)	60 (47%)	
Calcification				0.965
Absent	142 (68%)	55 (69%)	87 (67%)	
Present	67 (32%)	25 (31%)	42 (33%)	
Vascularity				0.427
Absent	83 (40%)	35 (44%)	48 (37%)	
Present	126 (60%)	45 (56%)	81 (63%)	
ER	90 (80, 90)	90 (58, 90)	90 (80, 90)	0.001
PR	80 (10, 90)	80 (2, 90)	80 (40, 90)	0.040
KI67	20 (10, 30)	30 (10, 40)	20 (10, 30)	0.002

Note: L, Maximum diameter; S, Shortest path; Middle, anteroposterior diameter; HER2, human epidermal growth factor receptor 2; ER, estrogen receptor; PR, progesterone receptor; KI67, marker of proliferation Ki-67; T1, tumor stage 1; T2, tumor stage 2.

set as the threshold to define statistical significance. For descriptive statistics, continuous variables were presented as mean ± standard deviation, whereas categorical variables were expressed as median (interquartile range) and frequency (%). The Mann-Whitney U test was employed to analyze continuous variables, while either the chi-squared test or Fisher's exact test was used for categorical variables, depending on the stratification of the dataset and its suit-

Table 2. Univariable and multivariable analyses of clinical characteristics and clinicopathologic features of patients in the training set (n = 155).

Variable	Univariable analysis			Multivariable analysis		
	OR	95% CI	*p*-value	OR	95% CI	*p*-value
Clear	0.333	0.129–0.862	0.057	-	-	-
KI67	1.002	0.994–1.010	0.697	-	-	-
Height	1.002	1.001–1.004	0.020	1.001	0.947–1.058	0.971
Age	1.006	1.001–1.011	0.049	0.982	0.957–1.008	0.245
ER-positivity	1.007	1.004–1.010	0.001	1.019	1.007–1.033	0.012
Weight	1.007	1.002–1.011	0.021	0.981	0.918–1.048	0.630
PR-positivity	1.007	1.004–1.011	0.002	1.000	0.990–1.010	0.971
Middle	1.011	0.990–1.031	0.381	-	-	-
L	1.014	1.003–1.026	0.046	0.996	0.969–1.024	0.828
S	1.014	0.999–1.030	0.128	-	-	-
T	1.077	0.688–1.685	0.786	-	-	-
Direction	1.196	0.889–1.611	0.322	-	-	-
Margin	1.229	0.845–1.786	0.366	-	-	-
Posteriorecho	1.314	0.908–1.900	0.223	-	-	-
Echo	1.339	1.002–1.791	0.098	-	-	-
Bloodflow	1.350	0.958–1.902	0.150	-	-	-
Shape	1.460	1.116–1.912	0.021	2.134	0–17,378.69	0.890
Location	1.484	1.012–2.175	0.089	-	-	-
Calcification	1.941	1.188–3.171	0.026	1.322	0.696–2.514	0.474
N	2.333	1.323–4.116	0.014	1.452	0.715–2.948	0.386
History	2.500	0.631–9.895	0.273	-	-	-

Note: CI, confidence interval; OR, odds ratio; N, lymph node metastasis; T, clinical tumor stage.

ability. In addition, the Analysis of Variance (ANOVA) and Kruskal-Wallis H tests were employed when comparing three or more groups.

3. Results

3.1 Patient Clinical Results

This investigation comprised 209 eligible patients stratified into training (n = 155) and test (n = 54) cohorts. Clinical profiling included patient age, anthropometric parameters (height/weight), tumor diameter, and spatial distribution (Table 1). Univariate logistic regression identified significant associations between HER2-low status and age (odds ratio [OR] = 1.006, p = 0.049), height (OR = 1.002, p = 0.020), weight (OR = 1.007, p = 0.021), lymph node metastasis (OR = 1.014, p = 0.046), ER-positivity (OR = 1.007, p = 0.001), and progesterone receptor (PR)-positivity (OR = 1.007, p = 0.002). Multivariate adjustment revealed that ER status was the only independent predictor of HER2-low status (OR = 1.019, 95% confidence interval [CI]: 1.007–1.033; p = 0.012) (Table 2). The clinical prediction model demonstrated limited discriminative capacity in the test set (AUC = 0.594, 95% CI: 0.448–0.740). The comprehensive performance evaluation, including calibration and decision curves for all models in both training and test sets, is presented in Fig. 3.

3.2 Intratumoral and Peritumoral Feature Selection and Model Construction

A total of 3320 radiomic signatures were extracted from within the intratumoral region and the 1 mm and 2 mm ROIs in the peritumoral region. These included 1651 intratumoral features and 1651 peritumoral features. LASSO dimensionality reduction was used to select 30 features from the intratumoral region, and 19 and 24 features from the 1 mm and 2 mm peritumoral regions, respectively. The selected features and their corresponding coefficients for each region are visualized in Fig. 4A–C. A composite radiomics model was developed by integrating the intratumoral features with the peritumoral features extracted from both the 1 mm and 2 mm regions. This model was designed to quantitatively assess the differentiation of HER2-low from HER2-zero BC. The performance metrics of these models, as evaluated in the training and test cohorts, are detailed in Table 3.

The radiomics model based on intratumoral features alone demonstrated an AUC of 0.730 (95% CI: 0.647–0.814) in the training set, and 0.649 (95% CI: 0.489–0.808) in the test set (Fig. 4D). In comparison, the peritumoral radiomics model combining intratumoral features with a 1 mm ROI showed enhanced performance, achieving AUC values of 0.852 (95% CI: 0.788–0.916) in the training set and 0.868 (95% CI: 0.771–0.965) in the test set (Fig. 4E). Expansion of the peritumoral ROI to 2 mm while main-

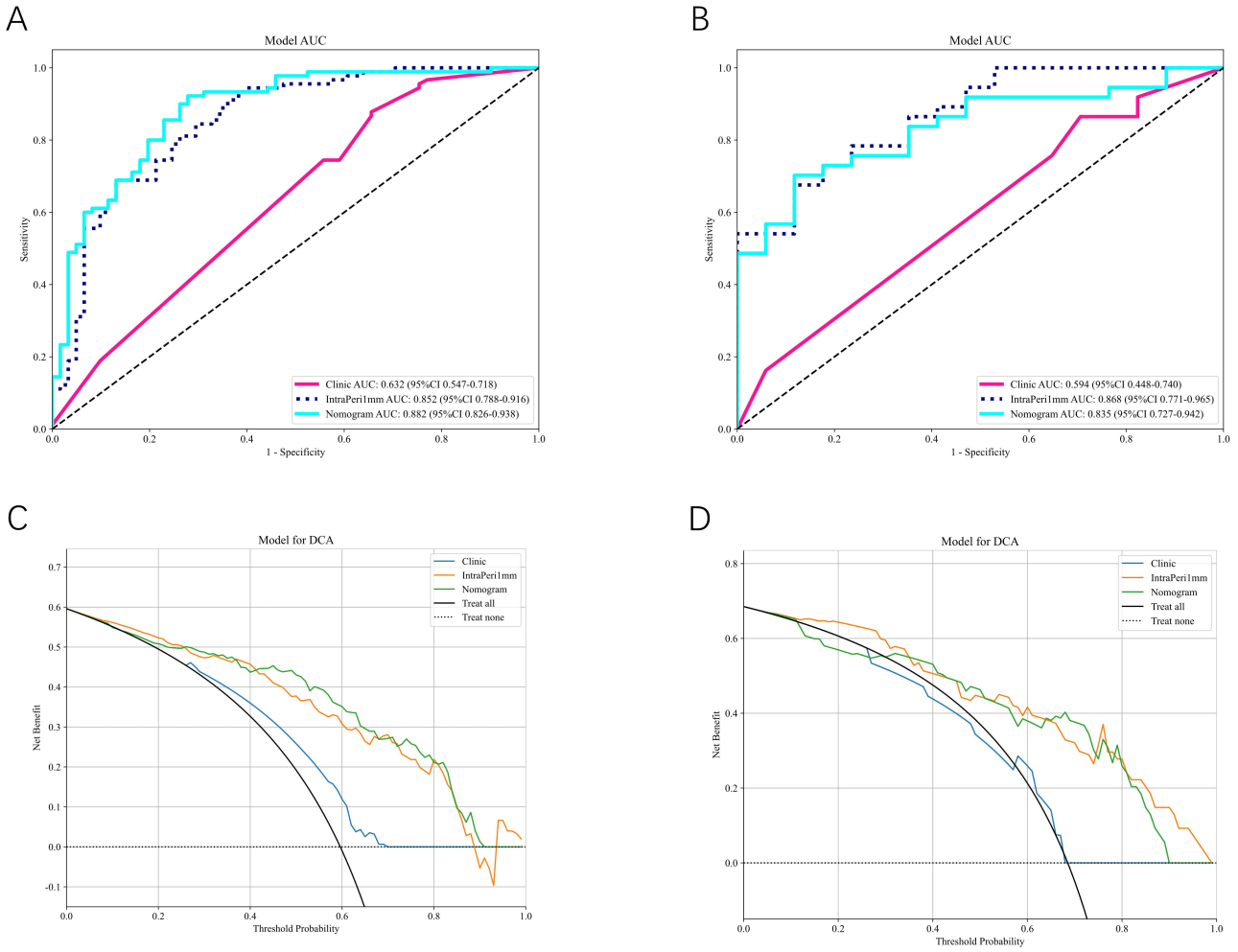

Fig. 3. Model performance comparison. (A,B) Calibration curves for the clinical model, radiology model, and column chart model in the training (A) and test (B) sets. (C,D) Decision curves for the clinical model, radiology model, and column chart model in the training (C) and test (D) sets.

taining integration of intratumoral features resulted in the model exhibiting superior training set performance, with an AUC of 0.918 (95% CI: 0.876–0.959). However, a substantial performance degradation was observed in the test set, with an AUC of just 0.509 (95% CI: 0.357–0.662) (Fig. 4F).

These findings suggest that incorporation of peritumoral regions into radiomics analysis results in better predictive performance compared to using intratumoral analysis alone. Additionally, by comparing results from different peritumoral sizes, the peritumoral region with a 1 mm ROI, in combination with the intratumoral model, was found to have the best predictive performance.

3.3 Construction of the Combined Model

We next developed a comprehensive prediction model by integrating intratumoral and 1 mm peritumoral US imaging-derived radiomic features with clinical risk factors. This model led to the creation of a nomogram, depicted in Fig. 5, which was designed to discriminate between HER2-low and HER2-zero BCs. Notably, the VIFs of the predictors in the nomogram, which included clinical risk factors and radiomic features, ranged from 1.039 to 1.179, indicating the absence of multicollinearity among the variables. The model performance was assessed based on its AUC value. In the training set, the model exhibited an AUC of 0.882 (95% CI: 0.826–0.938), while in the test set the AUC was 0.835 (95% CI: 0.727–0.942). DCA revealed that nomograms incorporating clinical features, intratumoral and 1 mm peritumoral US imaging radiomic features were capable of differentiating HER2-low from HER2-zero BC.

Notably, the results indicated the diagnostic ability of the nomogram was marginally lower than that of the intratumoral and 1 mm peritumoral radiomics models.

4. Discussion

In this study, we developed a predictive model integrating clinical parameters and grayscale US-based intratumoral and peritumoral radiomic features to differentiate

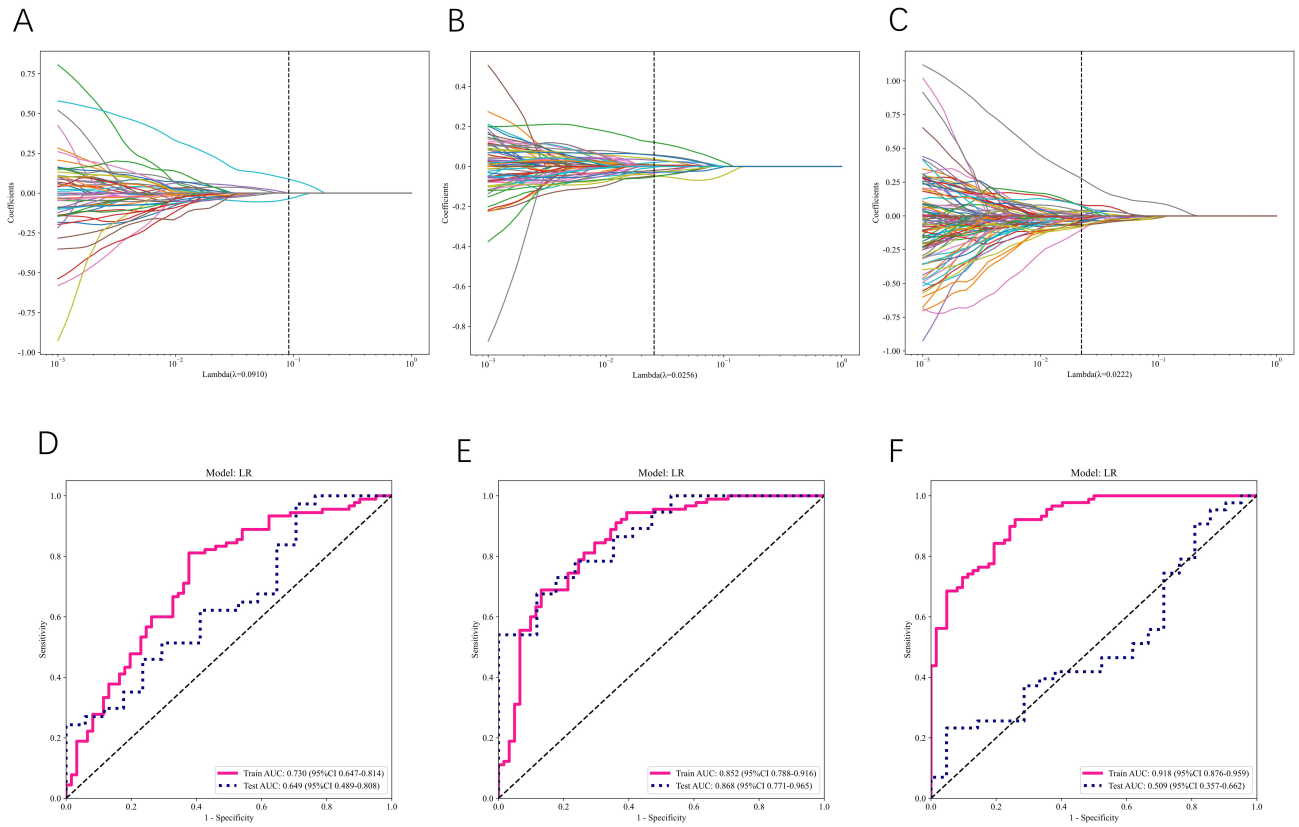

Fig. 4. AUC plots of the radiomics model for the area in and around the tumor. (A) Radiological characteristics of the intratumoral area selected by LASSO. (B) Radiomics characteristics of the 1 mm peritumoral area selected by LASSO. (C) Radiomics characteristics of the 2 mm peritumoral area selected by LASSO. (D–F) ROC curves of intratumoral (D), 1 mm peritumoral (E) and 2 mm peritumoral (F) regions.

HER2-low from HER2-zero status in BC patients. Previous studies that concentrated on the imaging profiles of HER2-negative and HER2-positive cases reported diagnostic performance ranging from moderate to substantial accuracy [23,24]. However, until recently, HER2-low BC has often been under-represented in clinical research. The emergence of new antibody-drug conjugates (ADCs) targeting HER2 has once again drawn attention to HER2-low tumors [25]. A subset of BCs featuring low HER2 expression level and lacking significant *ERBB2* amplification is designated as "HER2-low". These tumors are characterized by an IHC score for HER2 of either 1+ or 2+, and a negative test result for *ERBB2* in ISH [26]. Given their different biological phenotype, therapeutic responses, and clinical outcomes, HER2-low BC should be considered a novel BC subtype separate from HER2-zero (IHC 0) BC. In future, the definition of HER2 status in BC is likely to include three categories, comprising HER2-positive, HER2-negative, and HER2-low, of which the latter subgroup may benefit from targeted therapy regimens.

Bian *et al.* [17] devised a multiparametric, MRI-based radiomics approach to discriminate HER2-zero tumors from HER2-positive tumors. The former were further subdivided into HER2-low and HER2-zero subtypes, achieving an acceptable AUC of 0.81. Yin *et al.* [16] also reported a DCE-MRI radiomics model to differentiate these two subtypes, achieving an AUC of 0.78. While their work demonstrated the potential of radiomics for HER2 subtyping, their approach requires specialized equipment and contrast administration, thus limiting widespread clinical adoption. In contrast, our US-based model not only achieves superior performance (AUC = 0.882), but also overcomes these practical constraints through the inherent advantages of US technology. Moreover, the performance of our model surpasses that of the nomogram model by Yin *et al.* [16]. US is one of the primary modalities for clinical BC screening, with considerable merit beyond its extensive availability and cost-effectiveness compared to MRI. The ubiquitous availability of US in primary care clinics and community hospitals addresses a critical accessibility gap. Whereas MRI scanners are predominantly available in tertiary care centers (present in only 18% of Chinese county-level hospitals according to recent surveys), US systems are present in over 95% of healthcare facilities. This is particularly important for the detection of HER2-low, as such patients often present initially at community healthcare settings before specialist referral.

Table 3. Diagnostic performance of the radiomics model.

Set	Signature	AUC	95% CI	PPV	NPV	Sensitivity	Specificity	Accuracy
Train	Clinic	0.632	0.547–0.718	0.661	0.636	0.867	0.344	0.656
	Intra	0.730	0.647–0.814	0.758	0.679	0.800	0.623	0.728
	IntraPeri 1 mm	0.852	0.788–0.916	0.884	0.646	0.678	0.869	0.755
	IntraPeri 2 mm	0.918	0.876–0.959	0.835	0.852	0.910	0.742	0.841
	Nomogram	0.882	0.826–0.938	0.828	0.846	0.911	0.721	0.834
Test	Clinic	0.594	0.448–0.740	0.718	0.400	0.757	0.353	0.630
	Intra	0.649	0.489–0.808	0.745	0.714	0.946	0.294	0.741
	IntraPeri 1 mm	0.868	0.771–0.965	0.923	0.536	0.649	0.882	0.722
	IntraPeri 2 mm	0.509	0.357–0.662	0.900	0.370	0.209	0.952	0.453
	Nomogram	0.835	0.727–0.942	0.926	0.556	0.676	0.882	0.741

Note: Intra, intratumoral features; Peri, peritumoral features; PPV, positive predictive value; NPV, negative predictive value; Nomogram, combined clinical features, intratumoral and 1 mm peritumoral US imaging features.

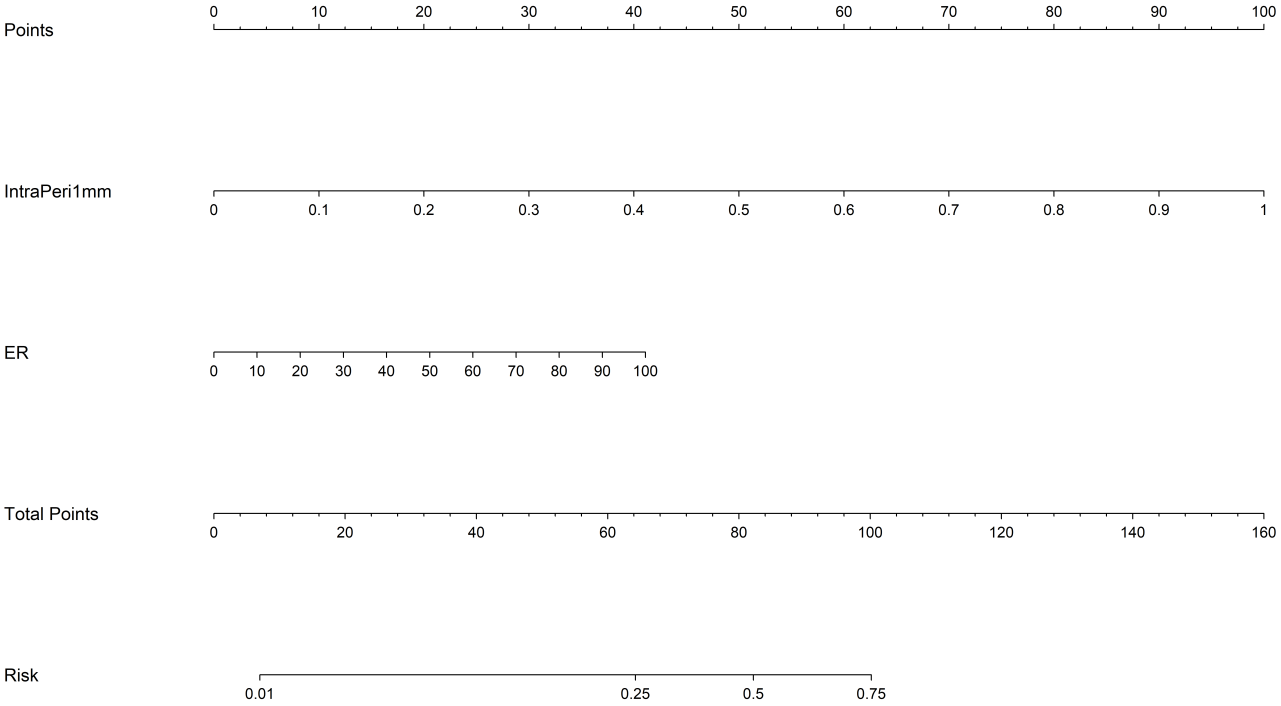

Fig. 5. Construction of the nomogram model, incorporating clinical features with intratumoral and peritumoral US imaging-derived radiomic features. ER, ER-positivity.

Previous studies on radiomics in BC molecular typing have focused on deriving information and features from the intratumoral region to differentiate between HER2-low and HER2-zero BC [27–29]. However, there is now increasing evidence for a substantial correlation between the tumor microenvironment (TME) and cancer cell behavior, including unrestricted proliferation and immune evasion. This implies that peritumoral regions may also furnish valuable information [30]. Therefore, in the present study we used IHC and FISH to determine HER2 status, combined the results from intratumoral and adjacent peritumoral regions of BC, designed a comprehensive radiomics and clinical model by applying machine learning algorithms, and compared the diagnostic accuracy of different models for discriminating HER2-low from HER2-zero BC. Our integrated model demonstrated robust discriminative performance, with AUC values of 0.882 (95% CI: 0.826–0.938) in the training cohort and 0.835 (95% CI: 0.727–0.942) in the validation cohort. These results indicate that an intratumoral and peritumoral radiomics model, combined with the clinical model, can effectively distinguish between HER2-low and HER2-zero BC subtypes.

Furthermore, this study found the clinical model exhibited relatively poor performance when compared to the clinical model combined with the intratumoral and peritumoral radiomics model, as well as to the nomogram model.

The latter two models demonstrated a high discriminative capacity between HER2-low and HER2-zero BCs. The AUC of the clinical model in this study was 0.594, which is considerably lower than the 0.866 reported by Chen *et al*. [27] for their clinical model. These authors included ER status, PR status, lymph node metastasis and internal echo to construct their clinical model after multivariate analysis, whereas the present study included only the ER status. The difference in AUC value may also be partly due to the limited sample size of our study. This led to a wide distribution of clinical data, causing certain relevant factors to be excluded following multi-factor screening. In future investigations, we plan to expand the cohort size to enhance the generalizability and robustness of our model. Notably, the highest diagnostic performance in the test set was not achieved by the nomogram model. Although this model incorporated both clinical and radiomic data, the AUC was 0.835 (95% CI: 0.730–0.940). Instead, the intratumoral and peritumoral radiomic model exhibited superior diagnostic efficacy, achieving an AUC of 0.868 (95% CI: 0.770–0.970). Critically, the high positive predictive value (PPV = 0.923) of our 1 mm intra-peri-tumoral model signifies excellent reliability for the confirmation of HER2-low status, thereby strengthening the indication for biopsy. Conversely, the moderate negative predictive value (NPV = 0.536) suggests that a negative result does not independently rule out the target condition, highlighting the need to integrate this tool with other clinical assessments for comprehensive decision-making.

This study focused on the 1 mm and 2 mm peritumoral regions for feature extraction. Nevertheless, uncertainties persist concerning the most appropriate delineation of the peritumoral region in BC. To date, a globally recognized gold standard for defining the peritumoral region in this specific clinical scenario is still lacking. The adoption of multi-scale, fixed-distance zones (0 mm, 1 mm, 2 mm) in the current study was based on existing findings in the field of BC radiomics and research into the TME, as well as validation results from our own study. The goal of this design is to strike a balance between capturing biologically relevant information (e.g., immune infiltration, neovascularization in the TME) and ensuring practical feasibility in clinical imaging analysis. Zhao *et al*. [31] provided compelling evidence for the utility of multi-scale peri-tumoral regions in predicting lympho-vascular invasion (LVI) in BC via DCE-MRI. Their multi-institutional study of 496 invasive BC cases involved the construction of models targeting 0–1 mm, 1–3 mm, and 3–5 mm peritumoral regions. The 0–1 mm peritumoral region contributed the highest weight coefficient in their fusion models [31]. After confirming 1 mm as the basic margin, we investigated the concept of multi-scale peritumoral margin validation, expanded the margin outward using 1 mm as the minimum unit, and sequentially designed larger peritumoral margins of 2 mm and 3 mm. We then constructed the respective radiomics models and tested their efficacy. However, the efficacy of models with 2 mm and larger peritumoral margins was all inferior. The AUC value, sensitivity, and specificity of the 2 mm margin model were significantly lower compared with the 1 mm model, while the efficacy of models with 3 mm margins or greater was even lower. In summary, the decisions regarding margin size in our study and the overall scope of this discussion are based on existing findings from previous BC peritumoral studies, combined with validation from our own experimental data, giving rise to the final scheme.

The 1 mm region is considered optimal, as the isolated peritumoral region often lacks sufficient data to adequately reflect the nuances of BC aggressiveness and US signal transmission. Moreover, the 2 mm region may contain excessive normal breast tissue, reducing the distinction between HER2-low and HER2-zero BC types. For example, in the final characteristics, "peri_wavelet_HLL_firstorder_Mean" reflects the average gray intensity of the peritumoral region post-wavelet transformation. Biologically, a higher value for this feature may indicate more prominent abnormal signals (e.g., inflammation or fibrosis) in HER2-low peritumoral tissues. Inflammation in the TME can attract immune cells that release cytokines to promote tumor growth and angiogenesis, while fibrosis forms a rigid extracellular matrix facilitating tumor cell invasion. In contrast, HER2-zero tumors show relatively homogeneous signals in the peritumoral region, with the difference facilitating subtype differentiation and providing insights into the distinct biological behaviors of this tumor subtype. "Intra_exponential_glszm_ZoneVariance" characterizes the variability in size of intratumoral homogeneous regions. Its negative weight implies that HER2-low tumors are likely to have more uniform intratumoral zone distribution. In contrast, HER2-zero tumors exhibit higher intratumoral heterogeneity, which is closely linked to tumor prognosis and treatment response, and may be associated with necrotic or cystic regions. Necrotic areas often indicate a more aggressive tumor phenotype, arising when rapid tumor growth outpaces blood supply, making this feature a valuable biological marker for distinguishing the two subtypes. "Peri_wavelet_LHL_glcm_Idn" quantifies the local homogeneity of peritumoral tissue via inverse difference normalization. A negative value for this characteristic indicates higher heterogeneity in the HER2-low peritumoral micro-environment, possibly due to mixed fibrosis or inflammation. This can alter tumor-stroma interactions, thereby affecting tumor cell motility and survival. Tumor-stroma cross-talk, including immune cell infiltration and angiogenesis, closely correlates with HER2 expression. Such interactions are concentrated in the area adjacent to the tumor, providing the biological signals needed to discriminate between HER2 subtypes in our US radiomics model [30,32]. The peritumoral micro-environment is a critical hub for immunosuppressive cell interactions (e.g., cancer-associated fibroblast (CAF)-mediated T-cell inhibi-

tion, tumor-associated macrophage (TAM)-induced therapy resistance). The micro-environmental differences between HER2 subtypes are precisely what is targeted by our peritumoral radiomics model [33]. The choice of 1 mm, rather than a broader margin, avoids diluting these tumor-specific signals. Expansion beyond 1 mm, as in the 2 mm model, increases the proportion of normal breast tissue (e.g., mammary ducts, adipose tissue) that is unrelated to tumor-stroma interactions, which is likely to explain the observed degradation in the performance of the test set (AUC = 0.509). The findings of this research support the practicality of peritumoral characteristics in US-based radiomics. Furthermore, the clinical workflow integration of our US radiomics model offers additional practical benefits. Unlike MRI which requires separate scheduling, US can be performed during routine diagnostic or biopsy procedures without additional patient visits, thus reducing diagnostic delays and allowing immediate clinical decision-making. This is particularly valuable for time-sensitive cases. Together, these advantages suggest our US-based approach may be a transformative solution for the detection of HER2-low BC in diverse clinical settings, from resource-limited rural clinics to advanced cancer centers. This should help address critical barriers to the widespread implementation of precision diagnostics in BC care.

To address the inherent subjectivity of manual ROI segmentation, we implemented rigorous measures to minimize operator-dependent variability. Prior to formal segmentation, each participating radiologist (n = 3) completed standardized training using 15 calibration cases that were excluded from the main cohort. This established consensus on critical parameters, including boundary definitions for irregular margins, protocols for heterogeneous echo patterns, and standardized ITK-SNAP software settings (version 3.8.0; http://www.itksnap.org/; developed by Paul A. Yushkevich, University of Pennsylvania, Philadelphia, PA, USA). The segmentation process employed a dual-observer design with two radiologists (each with $>$10 years of breast US experience) performing blinded annotations without access to pathological results. Inter-operator consistency was quantitatively verified using ICC on 30 randomly selected images, with a threshold of $>$0.75 for satisfactory agreement. Automated expansion of peritumoral regions (1 mm and 2 mm) and radiomic feature extraction/selection were conducted via the Pyradiomics platform with fixed parameters to ensure standardization. These multi-step quality control measures encompassed pre-segmentation training, dual-observer blinded annotation, objective ICC verification, and automated post-processing. Collectively, they systematically mitigated subjectivity, enhanced the reliability of our radiomic features, and strengthened the performance of our model in discriminating between HER2-low and HER2-zero BC.

Limitations

This study had several limitations that should be acknowledged. Firstly, a single-center retrospective design was adopted, where all enrolled cases were sourced from only one institution. We plan to mitigate this constraint by increasing the sample size and employing a multicenter study framework. Second, the extraction of all radiomics features based on manually delineated ROIs can be subjective. Despite the use of a double depiction method to ensure consistency, potential biases may still exist. To alleviate this limitation, features with a low ICC can be excluded to enhance robustness. At the same time, automatic algorithms based on deep learning can be employed in future to improve segmentation accuracy. This problem can be addressed by implementing artificial intelligence to automatically delineate ROI areas.

5. Conclusions

This study is the first attempt to investigate the utility of US-derived intratumoral and peritumoral features in radiomic analysis to discriminate between HER2-low and HER2-zero BC. Furthermore, the intra-peri-tumoral radiomic model developed in this study provides an auxiliary diagnostic tool to support the development of neoadjuvant chemotherapy protocols, and decreases the need for invasive biopsy procedures in BC patients. Our results confirm that peritumoral features harbor crucial information regarding the tumor itself, thereby justifying their inclusion in future radiomic research.

Abbreviations

BC, breast cancer; US, ultrasound; BI-RADS, Breast Imaging-Reporting and Data System; ROC, receiver operating characteristic curve; CI, confidence interval; AUC, area under the curve; IQR, interquartile range; FISH, fluorescence *in situ* hybridization; HER2, human epidermal growth factor receptor 2; IHC, immunohistochemistry; OR, odds ratio.

Availability of Data and Materials

The datasets used and analyzed during the current study are available from the corresponding authors on reasonable request.

Author Contributions

MNS designed the research study, conceived the radiomics model framework, and drafted the initial manuscript. SJM, ZBH and XHZ performed ultrasound image acquisition and preliminary quality control, ensuring compliance with imaging standards. HYW and HTT extracted clinical and pathological data from patient records, and verified data accuracy. SZT and MYW participated in manual ROI segmentation of ultrasound images, and assisted in validating inter-operator consistency via ICC

analysis. CYX conducted radiomic feature preprocessing and LASSO regression-based feature selection using Pyradiomics and R software. JFX, FJD and LPM supervised the study design and interpreted the statistical results. FJD and LPM are the corresponding authors and the guarantor of the integrity of the entire study. All authors contributed to editorial changes in the manuscript. All authors read and approved the final manuscript. All authors have participated sufficiently in the work and agreed to be accountable for all aspects of the work.

Ethics Approval and Consent to Participate

This study was conducted in accordance with the Declaration of Helsinki and was approved by the institutional review board of the First Affiliated Hospital, Southern University of Science and Technology, Shenzhen People's Hospital (LL-KY-2022479-02). This study obtained the informed consent of all patients. All methods were carried out in accordance with relevant guidelines and regulations.

Acknowledgment

Some of our experiments were carried out on Python technology provided by the LySono Research Platform. We thank LySono Team' s help in this research.

Funding

This research received no external funding.

Conflict of Interest

The authors declare no conflict of interest.

References

[1] Bray F, Laversanne M, Sung H, Ferlay J, Siegel RL, Soerjomataram I, *et al*. Global cancer statistics 2022: GLOBOCAN estimates of incidence and mortality worldwide for 36 cancers in 185 countries. CA. 2024; 74: 229–263. https://doi.org/10.3322/caac.21834.

[2] Fehrenbacher L, Cecchini RS, Geyer CE, Jr, Rastogi P, Costantino JP, Atkins JN, *et al*. NSABP B-47/NRG Oncology Phase III Randomized Trial Comparing Adjuvant Chemotherapy With or Without Trastuzumab in High-Risk Invasive Breast Cancer Negative for HER2 by FISH and With IHC 1+ or 2+. Journal of Clinical Oncology. 2020; 38: 444–453. https://doi.org/10.1200/JCO.19.01455.

[3] Giaquinto AN, Sung H, Newman LA, Freedman RA, Smith RA, Star J, *et al*. Breast cancer statistics 2024. CA: a Cancer Journal for Clinicians. 2024; 74: 477–495. https://doi.org/10.3322/caac.21863.

[4] Seshadri R, Firgaira FA, Horsfall DJ, McCaul K, Setlur V, Kitchen P. Clinical significance of HER-2/neu oncogene amplification in primary breast cancer. The South Australian Breast Cancer Study Group. Journal of Clinical Oncology. 1993; 11: 1936–1942. https://doi.org/10.1200/JCO.1993.11.10.1936.

[5] Choong GM, Cullen GD, O'Sullivan CC. Evolving standards of care and new challenges in the management of HER2-positive breast cancer. CA. 2020; 70: 355–374. https://doi.org/10.3322/caac.21634.

[6] Ge S, Wang B, Wang Z, He J, Ma X. Common Multiple Primary Cancers Associated With Breast and Gynecologic Cancers and Their Risk Factors, Pathogenesis, Treatment and Prognosis: A Review. Frontiers in Oncology. 2022; 12: 840431. https://doi.org/10.3389/fonc.2022.840431.

[7] Tarantino P, Hamilton E, Tolaney SM, Cortes J, Morganti S, Ferraro E, *et al*. HER2-Low Breast Cancer: Pathological and Clinical Landscape. Journal of Clinical Oncology. 2020; 38: 1951–1962. https://doi.org/10.1200/JCO.19.02488.

[8] Tarantino P, Viale G, Press MF, Hu X, Penault-Llorca F, Bardia A, *et al*. ESMO expert consensus statements (ECS) on the definition, diagnosis, and management of HER2-low breast cancer. Annals of Oncology. 2023; 34: 645–659. https://doi.org/10.1016/j.annonc.2023.05.008.

[9] Cheng X. A Comprehensive Review of HER2 in Cancer Biology and Therapeutics. Genes. 2024; 15: 903. https://doi.org/10.3390/genes15070903.

[10] Modi S, Jacot W, Yamashita T, Sohn J, Vidal M, Tokunaga E, *et al*. Trastuzumab Deruxtecan in Previously Treated HER2-Low Advanced Breast Cancer. The New England Journal of Medicine. 2022; 387: 9–20. https://doi.org/10.1056/NEJMoa2203690.

[11] Zhang H, Peng Y. Current Biological, Pathological and Clinical Landscape of HER2-Low Breast Cancer. Cancers. 2022; 15: 126. https://doi.org/10.3390/cancers15010126.

[12] Banerji U, van Herpen CML, Saura C, Thistlethwaite F, Lord S, Moreno V, *et al*. Trastuzumab duocarmazine in locally advanced and metastatic solid tumours and HER2-expressing breast cancer: a phase 1 dose-escalation and dose-expansion study. The Lancet. Oncology. 2019; 20: 1124–1135. https://doi.org/10.1016/S1470-2045(19)30328-6.

[13] Zhang G, Ren C, Li C, Wang Y, Chen B, Wen L, *et al*. Distinct clinical and somatic mutational features of breast tumors with high-, low-, or non-expressing human epidermal growth factor receptor 2 status. BMC Medicine. 2022; 20: 142. https://doi.org/10.1186/s12916-022-02346-9.

[14] Schettini F, Chic N, Brasó-Maristany F, Paré L, Pascual T, Conte B, *et al*. Clinical, pathological, and PAM50 gene expression features of HER2-low breast cancer. NPJ Breast Cancer. 2021; 7: 1. https://doi.org/10.1038/s41523-020-00208-2.

[15] Guo R, Lu G, Qin B, Fei B. Ultrasound Imaging Technologies for Breast Cancer Detection and Management: A Review. Ultrasound in Medicine & Biology. 2018; 44: 37–70. https://doi.org/10.1016/j.ultrasmedbio.2017.09.012.

[16] Yin L, Zhang Y, Wei X, Shaibu Z, Xiang L, Wu T, *et al*. Preliminary study on DCE-MRI radiomics analysis for differentiation of HER2-low and HER2-zero breast cancer. Frontiers in Oncology. 2024; 14: 1385352. https://doi.org/10.3389/fonc.2024.1385352.

[17] Bian X, Du S, Yue Z, Gao S, Zhao R, Huang G, *et al*. Potential Antihuman Epidermal Growth Factor Receptor 2 Target Therapy Beneficiaries: The Role of MRI-Based Radiomics in Distinguishing Human Epidermal Growth Factor Receptor 2-Low Status of Breast Cancer. Journal of Magnetic Resonance Imaging. 2023; 58: 1603–1614. https://doi.org/10.1002/jmri.28628.

[18] Chen R, Qi Y, Huang Y, Liu W, Yang R, Zhao X, *et al*. Diagnostic value of core needle biopsy for determining HER2 status in breast cancer, especially in the HER2-low population. Breast Cancer Research and Treatment. 2023; 197: 189–200. https://doi.org/10.1007/s10549-022-06781-3.

[19] Li R. Peritumoral Radiomics and Predicting Treatment Response. JAMA Network Open. 2020; 3: e2016125. https://doi.org/10.1001/jamanetworkopen.2020.16125.

[20] Bossuyt PM, Reitsma JB, Bruns DE, Gatsonis CA, Glasziou PP, Irwig L, *et al*. STARD 2015: An Updated List of Essential Items for Reporting Diagnostic Accuracy Studies. Clinical Chemistry. 2015; 61: 1446–1452. https://doi.org/10.1373/clinchem.2015.246280.

[21] Wolff AC, Hammond MEH, Allison KH, Harvey BE, Mangu PB, Bartlett JMS, *et al*. Human Epidermal Growth Factor Receptor 2 Testing in Breast Cancer: American Society of Clinical Oncology/College of American Pathologists Clinical Practice Guideline Focused Update. Journal of Clinical Oncology. 2018; 36: 2105–2122. https://doi.org/10.1200/JCO.2018.77.8738.

[22] Akinwande MO, Dikko HG, Samson A. Variance inflation factor: as a condition for the inclusion of suppressor variable(s) in regression analysis. Open Journal of Statistics. 2015; 5: 754.

[23] Fang C, Zhang J, Li J, Shang H, Li K, Jiao T, *et al*. Clinical-radiomics nomogram for identifying HER2 status in patients with breast cancer: A multicenter study. Frontiers in Oncology. 2022; 12: 922185. https://doi.org/10.3389/fonc.2022.922185.

[24] Xu A, Chu X, Zhang S, Zheng J, Shi D, Lv S, *et al*. Development and validation of a clinicoradiomic nomogram to assess the HER2 status of patients with invasive ductal carcinoma. BMC Cancer. 2022; 22: 872. https://doi.org/10.1186/s12885-022-09967-6.

[25] Modi S, Park H, Murthy RK, Iwata H, Tamura K, Tsurutani J, *et al*. Antitumor Activity and Safety of Trastuzumab Deruxtecan in Patients With HER2-Low-Expressing Advanced Breast Cancer: Results From a Phase Ib Study. Journal of Clinical Oncology. 2020; 38: 1887–1896. https://doi.org/10.1200/JCO.19.02318.

[26] Sonthineni C, Mohindra N, Agrawal V, Neyaz Z, Jain N, Mayilvagnan S, *et al*. Correlation of digital mammography and digital breast tomosynthesis features of self-detected breast cancers with human epidermal growth factor receptor type 2/neu status. South Asian Journal of Cancer. 2019; 8: 140–144. https://doi.org/10.4103/sajc.sajc_300_18.

[27] Chen J, Yin Y, Li G, Tian H, Ding Z, Mo S, *et al*. Integrated nomogram to predict HER2 expression in breast tumor: Clinical, Ultrasound, and Photoacoustic imaging approaches. European Journal of Cancer. 2024; 209: 114259. https://doi.org/10.1016/j.ejca.2024.114259.

[28] Cui H, Sun Y, Zhao D, Zhang X, Kong H, Hu N, *et al*. Radiogenomic analysis of prediction HER2 status in breast cancer by linking ultrasound radiomic feature module with biological functions. Journal of Translational Medicine. 2023; 21: 44. https://doi.org/10.1186/s12967-022-03840-7.

[29] Zhang X, Kong H, Liu X, Li Q, Fang X, Wang J, *et al*. Nomograms for predicting recurrence of HER2-positive breast cancer with different HR status based on ultrasound and clinicopathological characteristics. Cancer Medicine. 2024; 13: e70146. https://doi.org/10.1002/cam4.70146.

[30] Braman N, Prasanna P, Whitney J, Singh S, Beig N, Etesami M, *et al*. Association of Peritumoral Radiomics With Tumor Biology and Pathologic Response to Preoperative Targeted Therapy for HER2 (ERBB2)-Positive Breast Cancer. JAMA Network Open. 2019; 2: e192561. https://doi.org/10.1001/jamanetworkopen.2019.2561.

[31] Zhao Q, Zhang H, Xing W. Integrating Peritumoral and Intratumoral Radiomics with Deep Learning for Preoperative Prediction of Lymphovascular Invasion in Invasive Breast Cancer Using DCE-MRI. Technology in Cancer Research & Treatment. 2025; 24: 15330338251374945. https://doi.org/10.1177/15330338251374945.

[32] Park NJY, Jeong JY, Park JY, Kim HJ, Park CS, Lee J, *et al*. Peritumoral edema in breast cancer at preoperative MRI: an interpretative study with histopathological review toward understanding tumor microenvironment. Scientific Reports. 2021; 11: 12992. https://doi.org/10.1038/s41598-021-92283-z.

[33] Franzén AS, Raftery MJ, Pecher G. Implications for Immunotherapy of Breast Cancer by Understanding the Microenvironment of a Solid Tumor. Cancers. 2022; 14: 3178. https://doi.org/10.3390/cancers14133178.